Optical nonlinearity enhancement through correlated microstructure

M. F. Law, Y. Gu, and K. W. Yu
Department of Physics, The Chinese University of Hong Kong, Shatin, New Territories, Hong Kong, China
(Received 1 June 1998)

Optical nonlinearity is sensitively dependent on the microstructure in composites. In this paper, we analyze a model of correlated microstructure and examine the effect on the optical nonlinearity in the quasistatic limit. We perform numerical simulations on random-impedance networks that consist of metallic and dielectric bonds. The results show that the absorption peak can be separated from the nonlinearity enhancement peak so that the figure of merit may be increased. Thus, it may be possible to achieve an even larger optical nonlinearity than that reported in the literature. [S0163-1829(98)09043-2]

The optical properties of granular materials have attracted much interest. Many experiments were performed on composites of small metallic particles embedded in a dielectric host, in an attempt to sort out the physical origin of the anomalously large infrared absorption.[1–3] It was suggested that correlation and clustering effects may be the reason for the enhancement.[4] Recently, the optical nonlinearity of nanostructured composites has attracted much attention.[5] In particular, the metal clusters exhibit strong nonlinear optical response when they are structured on the nanometer scale, through the local-field and geometric-resonance effects, reflected in the spectral function.[6]

In this paper, we analyze a theoretical model of a correlated microstructure, which can be induced by thermal annealing, during which large clusters of like materials grow at the expense of small clusters. To examine the impact of a microstructure on the optical nonlinearity in the quasistatic limit,[7] we consider the displacement-field response of the form $\mathbf{D}=(\epsilon+\chi|\mathbf{E}|^2)\mathbf{E}$, where ϵ is the dielectric constant and χ is the third-order nonlinear susceptibility. It is convenient to introduce correlation through the power spectrum of the dielectric-constant fluctuations.[8] It was shown that long-range correlations can modify both the structural and dynamical properties of the percolating clusters.[9]

For numerical simulations, a composite medium is conveniently modeled by a random-impedance network. We shall focus only on two-dimensional networks that correspond to thin films. The generalization to three dimensions is straightforward.[10] Note that the problem of solving the electric field in a dielectric medium in the quasistatic limit is the same problem of solving that in a conducting medium. The thermodynamic limit corresponds to an infinite network size ($L\rightarrow\infty$), which can never be achieved due to the limitation of computer resources. In what follows, the finite-size effect will be justified.

We generate a correlated network by assigning a random number e ($0\leqslant e\leqslant 1$) to each site of the square lattice. For two neighboring sites with random numbers e_α and e_β, the following rule applies:[11] If $(e_\alpha+e_\beta)/2\leqslant p'$, then the bond between the sites is assigned with the value ϵ_1, otherwise the bond is assigned ϵ_2. The actual volume fraction p of ϵ_1 bonds is related to p' by $p=2p'^2$ for $p'\leqslant 1/2$ and $p=1-2(1-p')^2$ for $p'>1/2$. In this way, a site with a large e value is more likely to be surrounded by ϵ_2 bonds, and vice versa. As a result, larger clusters are formed; the actual p dependence of the weights of typical clusters can be calculated.[12] The enhancement of larger clusters will change the spectral density function, thereby having a pronounced effect on the optical absorption and nonlinearity.[6] These results are general and apply to various short-range correlation models.

Consider a random-impedance network between two parallel plates at unit potential difference, the effective linear and nonlinear response functions are given by[13]

$$\epsilon_e=\sum_\alpha \epsilon_\alpha \delta v_\alpha^2, \tag{1}$$

$$\chi_e=\frac{1}{L^2}\sum_\alpha \chi_\alpha|\delta v_\alpha|^2\delta v_\alpha^2, \tag{2}$$

where the summation is over all bonds and δv_α is the (generally complex) potential difference across the bond α, to be solved when all χ_α is being set to zero. We apply Kirchhoff's law to each of the nodes to obtain a set of simultaneous equations relating the potential of the node (v_ν) with those of its four neighboring ones (v_μ's):

$$\sum_{\mu=1}^{4}\epsilon_\mu(v_\mu-v_\nu)=0. \tag{3}$$

Writing the equations in a matrix form, we obtain a matrix $\mathbf{M}$ of size $L(L-1)\times L(L-1)$; $\mathbf{M}$ consists of nonzero elements along the five diagonals. This property helps us to optimize the calculation of the inverse $\mathbf{M}^{-1}$. The effective response is obtained by taking an ensemble average over a sufficiently large number of samples.

Below we shall use the spectral representation,[14,15] which is a rigorous mathematical formalism of the effective dielectric constant. It offers the advantage of separation of material parameters from the geometric information, which are contained in the spectral function $m(s)$. Moreover, $m(s)$ satisfies the sum rule [Eq. (5) below], which implies that an increase of $m(s)$ in some region must be balanced by a decrease of that in the other region. Hence, the absorption is directly linked to the behavior of $m(s)$. We calculate $m(s)$ via the limiting process[6]

 ©1998 The American Physical Society

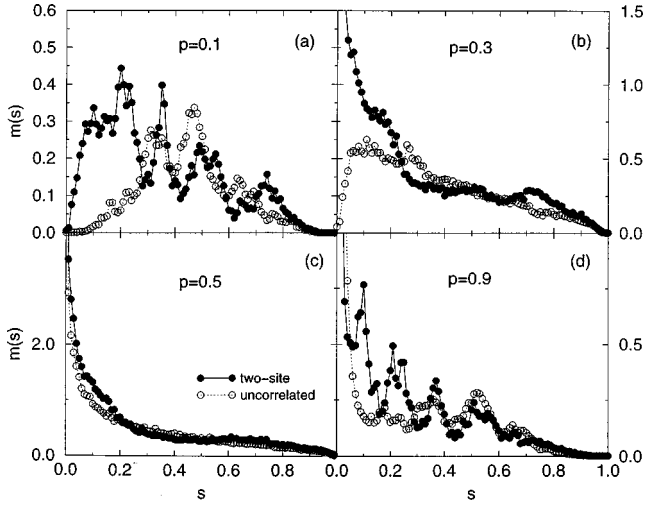

FIG. 1. The spectral function of correlated networks plotted as a function of s. (a) $p=0.1$, (b) $p=0.3$, (c) $p=0.5$, and (d) $p=0.9$. Results for the uncorrelated networks are plotted for comparison.

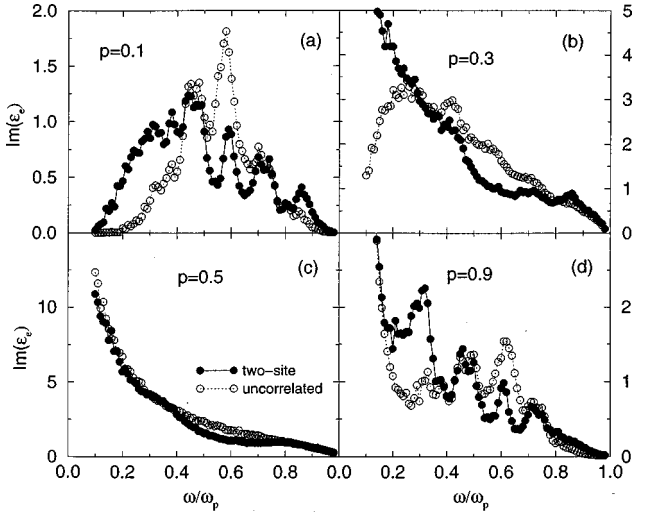

FIG. 2. The absorption $\mathrm{Im}(\epsilon_e)$ plotted against frequency ω. (a) $p=0.1$, (b) $p=0.3$, (c) $p=0.5$, and (d) $p=0.9$.

$$m(s)=\lim_{\eta\to 0^+}-\frac{1}{\pi}\mathrm{Im}\ w(s+i\eta), \tag{4}$$

where $w=1-\epsilon_e/\epsilon_2$ and $s=\epsilon_2/(\epsilon_2-\epsilon_1)$. We choose the real part of s at 100 equally spaced values across the interval $0\leqslant s'\leqslant 1$ and the imaginary part $\eta=0.002$, which is small enough by checking the sum rule:

$$\int_0^1 m(s')ds'=p. \tag{5}$$

A smaller value of η or a finer spacing of s give the resonance spectrum in more detail. An alternative method for finding the spectral function is recently demonstrated in Ref. 15, in which Kirchhoff's equations are transformed into an eigenvalue problem via the (lattice) Green's-function formalism.

Consider a metal-dielectric composite in which ϵ_1 is metallic and ϵ_2 is dielectric.[16] The metallic response is assumed to obey the Drude free-electron model:

$$\epsilon_1(\omega)=1-\frac{\omega_p^2}{\omega(\omega+i\gamma)}, \tag{6}$$

where ω_p is the plasma frequency and γ is the damping constant. For metal, the plasma frequency $\omega_p\approx 10^{16}$, being in the ultraviolet. We choose $\gamma=0.01\omega_p$, which is the typical value of a good metal, and $\epsilon_2=1.77$, which is the dielectric constant of water for model calculations. In this work, only the metallic part is taken to be nonlinear,[17] i.e., $\chi_2=0$.

We performed numerical simulations on various network sizes. After comparing the results from $L=10$ and 12, we conclude that $L=12$ is sufficient for the present investigation. A further increase in the network size results in no significant difference. It is because the optical response arises from the geometric resonances, rather than from the percolating effects. Each data point represents an ensemble average over 1000 random samples of $L=12$.

In Fig. 1 we plot the spectral function $m(s)$ of the correlated network for the various volume fraction p of metallic bonds. The spectral function for the uncorrelated networks is also plotted for comparison. For $p=0.1$, the uncorrelated network is dominated by small clusters of a few bonds (the lattice-animal limit[15]). There are several pronounced peaks around $s=0.3$, 0.5, and 0.7, which represent geometric resonances by small clusters of up to two bonds.[15] However, in the correlated networks, larger clusters are significantly enhanced at the expense of smaller ones; we observed a significant enhancement of the spectral function in the small-s region. These results are in accord with those reported in Ref. 4. Since the sum rule [Eq. (5)] must be obeyed, the spectral function has to be decreased in the large-s region. As a result, the absorption spectrum will be redshifted.

For $p=0.3$, the metal bonds form larger clusters of various sizes. The spectral density becomes a broad continuous function and the pronounced peaks diminish in the range $0.3\leqslant s\leqslant 0.7$. For the correlated networks, the spectral function becomes large near $s=0$. It is evident that the correlation leads to a decrease of the (finite-size) percolation threshold (as compared to $p_c=0.5$ for the uncorrelated networks).

For larger p, e.g., $p=0.5$ and 0.9, the spectral function $m(s)$ becomes large towards $s=0$, signifying a percolation transition in both types of networks. However, a significant difference between the two networks still persists in the small-s region. The $p=0.5$ spectral density is a broad continuous function without any significant feature. However, for $p=0.9$, the pronounced peaks appear again in addition to the $s=0$ Drude peak. It is due to a formal relation between the $p=0.9$ and $p=0.1$ cases.

Next we examine the absorption, which is calculated from the imaginary part of the dielectric constant. In Fig. 2 we plot the absorption spectrum for various values of p. As evident from the figures, the small p results are well described by the lattice-animal limit, while the large p results are in accord with the presence of clusters of various sizes. The results are quite similar to those of the spectral function, i.e., a decrease of absorption in the visible range is predicted. Experimentally, a suppression of absorption is desirable for practical applications while we have demonstrated that it is possible to realize this suppression by correlated microstructures.

The optical nonlinearity is plotted in Fig. 3. For $p=0.1$,

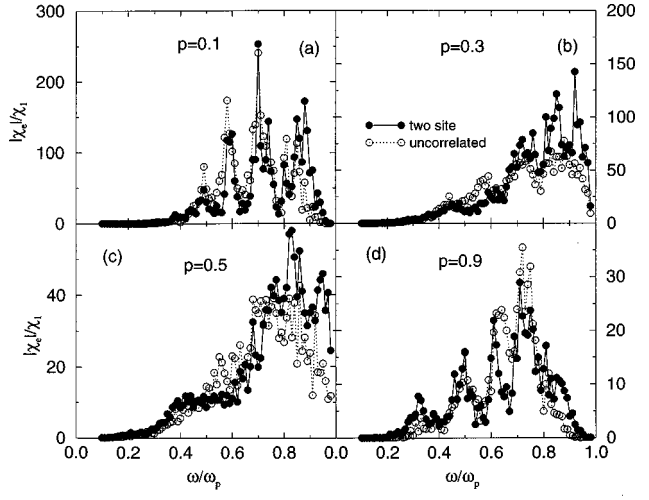

FIG. 3. The nonlinearity enhancement $|\chi_e|/\chi_1$ plotted against frequency ω. (a) $p=0.1$, (b) $p=0.3$, (c) $p=0.5$, and (d) $p=0.9$.

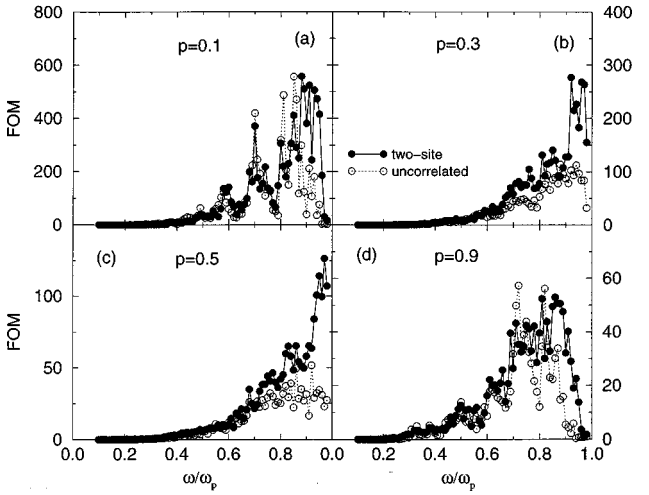

FIG. 4. The figure of merit plotted against frequency ω. (a) $p=0.1$, (b) $p=0.3$, (c) $p=0.5$, and (d) $p=0.9$.

the optical nonlinearity is found to be enhanced over the uncorrelated networks near $\omega/\omega_p=0.7$ and 0.9 as a result of correlation. However, from Fig. 2, the absorption near $\omega/\omega_p=0.9$ is also increased. Fortunately, for $\omega/\omega_p\approx 0.7$, the absorption is about the same for both networks. It is thus beneficial to introduce the correlation in this frequency region. For $p=0.3$, sharp resonances occur in the high-frequency region, resulting in a nonlinearity enhancement over the uncorrelated networks in the region $0.7<\omega/\omega_p<1$. From Fig. 2 again, we find that this region coincides with the region $(0.7<\omega/\omega_p<0.8)$, where the absorption is suppressed. Introducing the correlation in this frequency region is thus beneficial for practical purpose. For $p=0.5$, the nonlinearity is enhanced in the region $0.8<\omega/\omega_p<1$. For $p=0.9$, an enhancement can be found in the low-frequency region $\omega/\omega_p\approx 0.3$, as well as at frequencies near the plasma frequency $\omega=\omega_p$.

In order to illustrate the enhancement more clearly, we plot in Fig. 4 the figure of merit (FOM), defined as the ratio of the third-order nonlinear susceptibility to the absorption. For $p=0.1$, the FOM near $\omega/\omega_p\approx 0.7$ is found to be enhanced, in accordance with the above analysis of the optical nonlinearity. Moreover, the FOM near $\omega=\omega_p$ is more than double that of the uncorrelated networks. For $p=0.3$, a large FOM is obtained in the full range $\omega/\omega_p>0.6$, while the enhancement is a few times near the plasma frequency. The results for $p=0.5$ and 0.9 are quite similar. A larger FOM is generally obtained in the high-frequency region.

In this paper, the suppression of absorption and the concomitant enhancement of optical nonlinearity by correlated microstructures are demonstrated. The predicted enhancement of the present paper may have relevance to a recent optical-nonlinearity experiment on Au:SiO_2 composites,[18] in which a large enhancement was obtained for annealed samples. Through the separation of the absorption peak from the nonlinearity enhancement peak, it may be possible to achieve even larger optical nonlinearity than that reported in Ref. 18. Further numerical simulation on other short-range correlation models reveals that the correlated microstructure affects the optical nonlinearity enhancement in a similar way:[19] The absorption spectrum is redshifted while the optical nonlinearity is enhanced in the visible range. As a result, the FOM is enhanced. In closing, it is worth extending the present investigations to microstructures with the long-range correlation[9] or anisotropy.[19] We expect that such microstructures will have pronounced effects on the optical nonlinearity enhancement.

This work was supported by the Research Grants Council of the Hong Kong SAR Government. K.W.Y. acknowledges useful conversations with Professor Ping Sheng.

[1] D. B. Tanner, A. J. Sievers, and R. A. Buhrman, Phys. Rev. B **11**, 1330 (1975).

[2] C. G. Granqvist, R. A. Buhrman, J. Wyns, and A. J. Sievers, Phys. Rev. Lett. **37**, 625 (1976).

[3] R. P. Devaty and A. J. Sievers, Phys. Rev. Lett. **52**, 1344 (1984).

[4] X. C. Zeng, P. M. Hui, D. J. Bergman, and D. Stroud, Phys. Rev. B **39**, 13 224 (1989).

[5] See articles in *Nanostructured Materials: Clusters, Composites and Thin Films*, edited by V. M. Shalaev, ACS Symposium Series 679 (American Chemical Society, Washington, DC, 1997).

[6] K. P. Yuen, M. F. Law, K. W. Yu, and P. Sheng, Phys. Rev. E **56**, R1322 (1997).

[7] As we consider the short-range correlation in our model, it does not lead to very large clusters whose sizes are bigger than the wavelength of light and the quasistatic approximation can be employed. The quasistatic approximation can only become unjustified when the metal volume fraction is close to the percolation threshold when large metallic clusters exist.

[8] H. Makse, S. Havlin, H. E. Stanley, and M. Schwartz, Chaos Solitons Fractals **6**, 295 (1995).

[9] S. Prakash, S. Havlin, M. Schwartz, and H. E. Stanley, Phys. Rev.

A **46**, R1724 (1992).

[10] The simulation can be extended in a straightforward manner to three-dimensional networks by using the modified transfer-matrix method for calculating the electric field.

[11] S. Kirkpatrick, Rev. Mod. Phys. **45**, 574 (1973).

[12] Y. Gu (unpublished).

[13] D. Stroud and P. M. Hui, Phys. Rev. B **37**, 8719 (1988).

[14] D. J. Bergman and D. Stroud, in *Solid State Physics*, edited by H. Ehrenreich and D. Turnbull (Academic Press, New York, 1992), Vol. 146, p. 147.

[15] For discrete network models, see J. P. Clerc, G. Giraud, J. M. Luck, and Th. Robin, J. Phys. A **29**, 4781 (1996); see also Th. Jonckheere and J. M. Luck, *ibid.* **31**, 3687 (1998).

[16] Since suppression of absorption already occurs in the visible region (below the ultraviolet), we can ignore the absorption of the embedding dielectric medium. Nevertheless, the absorption of the embedding medium can be treated in a straighforward manner, using our network model.

[17] Although the optical nonlinearity of free electrons may be strongly frequency dependent in the visible regime, we compare the results of the correlated and uncorrelated networks at exactly the same frequency.

[18] H. B. Liao, R. F. Xiao, J. S. Fu, P. Yu, G. K. L. Wong, and P. Sheng, Appl. Phys. Lett. **70**, 1 (1997).

[19] M. F. Law, M. Phil. thesis, Chinese University of Hong Kong, 1998.